

# Leaky-mode resonant gratings on a fibre facet

Martin Vanek<sup>1</sup> · Jiri Ctyroky<sup>1</sup> · Pavel Honzatko<sup>1</sup> 

Received: 24 June 2017 / Accepted: 19 December 2017  
© The Author(s) 2018. This article is an open access publication

**Abstract** Numerical investigation shows that an optimised leaky-mode resonant diffraction gratings fabricated in Ta<sub>2</sub>O<sub>5</sub> layer deposited on the facet of an optical fibre can have a modal reflectance peak of more than 95%, 3 dB spectral bandwidth of about 50 nm and polarization extinction ratio of almost 18 dB. The grating is intended to be employed as a high-reflectance, wavelength- and polarization-dependent mirror in a fibre laser. We compare results of 2D and 3D modelling, investigate influence of grating parameters on spectral shape of modal reflectance and discuss fabrication tolerances.

**Keywords** Leaky-mode resonant gratings · Large mode area fibres · Finite-difference time-domain method

---

The authors acknowledge funding of this work by the Czech Science Foundation, Grant GAP15-07908S.

---

This article is part of the Topical Collection on Optical Wave and Waveguide Theory and Numerical Modelling, OQTNM 2017.

---

Guest Edited by Bastiaan Pieter de Hon, Sander Johannes Floris, Manfred Hammer, Dirk Schulz, Anne-Laure Fehrembach.

---

✉ Pavel Honzatko  
honzatko@ufe.cz

Martin Vanek  
vanek@ufe.cz

Jiri Ctyroky  
ctyroky@ufe.cz

<sup>1</sup> Institute of Photonics and Electronics, CAS, Chaberska 57, 182 51 Prague, Czech Republic

## 1 Introduction

In this paper we investigate leaky-mode resonant diffraction gratings (LMRG) used as a wavelength- and polarization-selective element in fibre lasers. Resonant leaky-mode diffraction gratings are phase-matching gratings allowing us to excite and simultaneously extract a guided mode of the adjacent waveguide. Their zero-order diffraction efficiency can be close to 100% in reflection. Leaky-wave resonance was recognized in some of Wood's diffraction anomalies by Hessel and Oliner (1965). Nevière et al. theoretically studied these anomalies in dielectric gratings combined with waveguides and related them to the existence of waveguide modes (Neviere et al. 1973). In 1985, Mashev and Popov experimentally demonstrated a resonance anomaly in the reflected zero diffraction order caused by the excitation of guided waves in a corrugated waveguide, which significantly increased the reflectance of the structure in a narrow wavelength band (Mashev and Popov 1985). Diffraction of a monochromatic plane wave by a surface-corrugated waveguide and by a substrate-corrugated waveguide was studied by Golubenko et al. (1985). A multiple interference model related to an intuitive ray picture and a second-order perturbation approach with a Green's function formulation were developed for thin dielectric waveguides by Sharon et al. (1997).

LMRGs were used as wavelength-selective elements in erbium-doped ZBLAN fluoride fibres operating in a spectral range of 2700–2900 nm (Johnson et al. 2012), in erbium-doped silica fibre laser at a wavelength of 1541 nm (Mehta et al. 2007), and in thulium-doped silica fibre lasers at a wavelength of about 2000 nm (Sims et al. 2011). A collimating optics was used in all these laser experiments in order to couple light from the optical fibre to the LMRG. Any of such intracavity elements negatively influences the threshold, slope efficiency, reliability and cost of high-power fibre lasers. It is therefore tempting to fabricate the LMRG directly on cleaved or polished fibre facets. Several technologies were examined for micromachining of fibre facets such as interference lithography (Yang et al. 2012), photolithography (Johnson et al. 2003), electron-beam lithography (Prasciolu et al. 2003), focused ion-beam milling (Schiappelli et al. 2004; Vanek et al. 2016), stamping (Sanghera et al. 2010; MacLeod et al. 2011), nano-imprint technology (Kostovski et al. 2009; Kanamori et al. 2013), two-photon polymerization 3D printing (Williams et al. 2011; Gissibl et al. 2016a, b), direct laser writing (Kowalczyk et al. 2014).

Here we report on a leaky-mode resonant diffraction grating that is intended to be employed as a high-reflectance, wavelength- and polarization-dependent mirror in a fibre laser. The grating is supposed to be milled into an oxide layer with high refractive index deposited on the fibre facet. The design of the diffraction grating is described in Sect. 2, optimization of the grating in Sect. 3, tolerance analysis in Sect. 4.

## 2 Leaky-mode resonant grating design

We design the LMRG for a specific use in high-power, thulium-doped fibre lasers such as shown in Fig. 1a. The resonator of the laser consists of a large mode area, double-clad, polarization maintaining thulium-doped fibre (PLMA-TDF), pump-signal combiner (PSC), and two mirrors. Laser diodes with multimode pigtailed are used for pumping the double-clad active fibre over the PSC. The low-reflectance mirror is formed by a perpendicularly cleaved output fibre of which the reflectance is 3.5% in accordance with Fresnel equations.

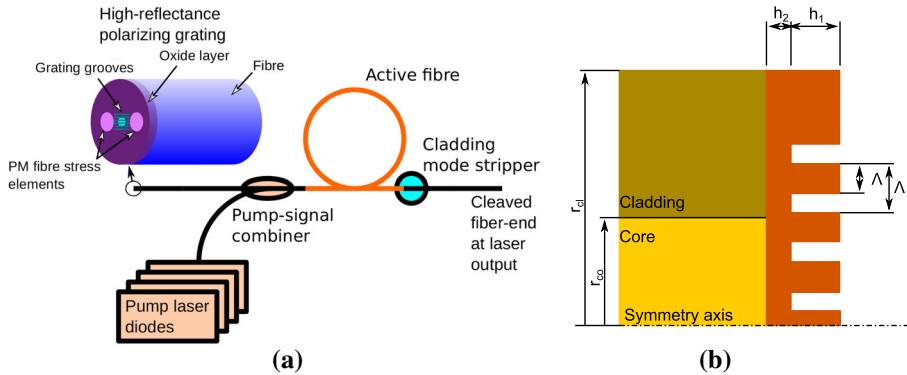


**Fig. 1** **a** Idea of LMRG application in a laser setup. **b** Optical fibre with resonant diffraction grating

The high-reflectance wavelength- and polarization-selective mirror is fabricated on the perpendicularly cleaved pigtail of the PSC in the form of an LMRG. We design the high-reflectance mirror so that it will have a resonance wavelength of 2000 nm, modal reflectance close to 100%, high polarization extinction ratio, and reasonably narrow bandwidth.

The fibre with the LMRG is shown in Fig. 1b. The single mode fibre has a core with radius  $r_{co}$  and refractive index  $n_{co}$ , cladding with radius  $r_{cl}$  and refractive index  $n_{cl}$ . An oxide layer with high refractive index  $n_{ox}$  and thickness  $h$  is deposited on the fibre facet. Finally, grating grooves with depth  $h_1$  are etched into the deposited layer. The sub-wavelength grating has period  $\Lambda$  and fill factor  $f$ . Throughout the paper, we assume parameters shown in Table 1. We neglect dielectric losses by setting extinction coefficients to zero.

Since the corrugated high-index layer is surrounded from both sides with lower-index media, it can be considered as a double-layer planar waveguide: a homogeneous layer with the thickness  $h_2$ , and a “segmented” layer with the thickness  $h_1$  and with somewhat lower polarization dependent refractive index according to the effective-medium theory (Lalanne and Hugonin 1998). This bi-layer can be thus considered as a planar leaky-wave waveguide perpendicular to the fibre. Light incident from the fibre is coupled in the 1-st diffraction orders of the grating into the waveguide in opposite directions. Light guided in the waveguide is back-reflected in the 2-nd diffraction orders of the grating and partially coupled out of the guiding layer in the 1-st diffraction orders. By proper adjustment of grating parameters the transmitted zeroth order can be suppressed by the destructive interference with the light coupled out of the guiding layer while the back-reflected zeroth order light is enhanced by constructive interference with the light coupled out of the layer in the backward direction. As a result, high spectrally selective back-reflection is achieved (Neviere et al. 1973; Golubenko et al. 1985).

Because of relatively high refractive index contrast of the structure, deep etch and only weakly subwavelength character of the grating, application of “rigorous” full-wave numerical modelling methods is required for the proper design of the grating.

**Table 1** Refractive indices and core radius used in the calculations

$n_{co}$	1.4428	$n_{cl}$	1.44	$n_{ox}$	1.906	$r_{co}$	12.5 $\mu\text{m}$
----------	--------	----------	------	----------	-------	----------	--------------------

The resonant wavelengths differ for TE and TM modes. We design the LMRG so that only TE mode resonance falls in the gain band of thulium-doped fibre. High extinction ratio of TE to TM polarization will allow laser operation with defined wavelength and polarization.

### 3 Leaky-mode resonance simulation

The finite-difference time-domain (FDTD) method is used to design and optimise the LMRG. We simulate propagation of a short optical pulse with finite bandwidth centred at a specific wavelength in the fibre using the open-source computer software MEEP (Oskooi et al. 2010). Only the fundamental fibre mode is excited in simulations. The pulse excites the leaky-mode resonance in the microstructure fabricated on the fibre facet. It should be noted that we analyse the excitation of the leaky mode by a short optical pulse just for convenience. The laser shown in Fig. 1a is assumed to operate in CW mode.

We calculate the transmission and reflection spectra by taking harmonic transforms of the time-domain fluxes through the measurement planes  $F_{g1}$  and  $F_{g2}$  situated before and behind the LMRG (Fig. 2). The plane  $F_{g1}$  is relatively far from the LMRG so that the diffracted light that is not coupled back to the fibre core can be absorbed in the perfectly matched layers (PML) surrounding the simulated area. The flux spectrum  $F_{1g}$  recorded in the simulations is, in fact, the difference of forward  $F_F$  and reflected  $F_R$  flux spectra,

$$F_{1g} = F_F - F_R. \tag{1}$$

We use a reference model of a fibre without any grating to find the forward flux spectrum  $F_F = F_{1f}$ . The reflected flux spectrum is

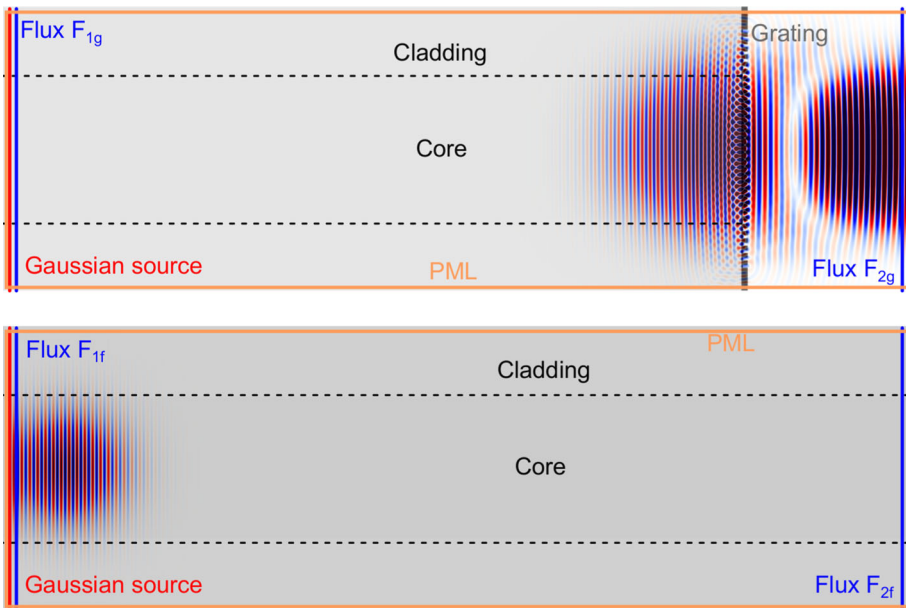


**Fig. 2** Model of the fibre with LMRG (top) and reference fibre (bottom) as used in the FDTD method. Perfectly matched layers (PML), source and flux planes are shown

$$F_R = F_{1f} - F_{1g}, \tag{2}$$

and the modal reflectance  $R_g$ , transmittance  $T_g$  and loss of the LMRG  $L_g$  are calculated as

$$R_g = F_R / F_{1f}, \tag{3}$$

$$T_g = F_{2g} / F_{2f}, \tag{4}$$

$$L_g = 1 - T_g - R_g. \tag{5}$$

In order to optimize gratings with limited computational resources, we resort to 2D-FDTD method for a 1D grating on the facet of a slab waveguide with the thickness equal to the diameter of the fibre. The simulations are performed with a resolution of 30 points/ $\mu\text{m}$  which corresponds to 60 points per wavelength in vacuum and roughly 30 points per wavelength in high refractive index oxide layer. The simulated area is  $128 \mu\text{m} \times 50 \mu\text{m}$  with PML thickness  $1.5 \mu\text{m}$ . The flux measurement planes are placed at a distance of  $5 \mu\text{m}$  from the left and right border. The source has Gaussian distribution both in time and space and is placed at a distance of  $4 \mu\text{m}$  from the left side of the simulated area. The modal width is estimated to be  $10.8 \mu\text{m}$  FWHM by minimizing loss in the reference waveguide without any grating. We assume a truncated periodic structure with  $N$  grooves, centered on the fibre axis. The number of grooves is set to 33 if not stated otherwise. Influence of the number of grating grooves on the modal reflectance is discussed in Sect. 4

We compare the 2D simulation results with full 3D simulations performed by Fourier modal method (3D-FMM) (Čtyroký 2012) in order to justify the use of such a simplified model. Very good agreement between modal reflectances calculated with 2D and 3D models was found (Fig. 3a). The whole modal reflectance curve calculated by 3D FMM is shifted by 2.0 nm to shorter wavelength compared to the curve calculated by the 2D-FDTD method. Both reflectance curves agree within 2.0% over the whole wavelength interval 1.9–2.1 nm, when this wavelength shift is taken into account. The peak reflectances, which are important for the laser performance, differ by 1.1%. Such a small uncertainty in the reflectance peak value will be negligible in experiment taking the fabrication tolerances into account.

We also compared modal reflectances calculated by the 2D-FDTD method with those calculated by the 2D-FMM and found that they are almost undistinguishable (Fig. 3b).

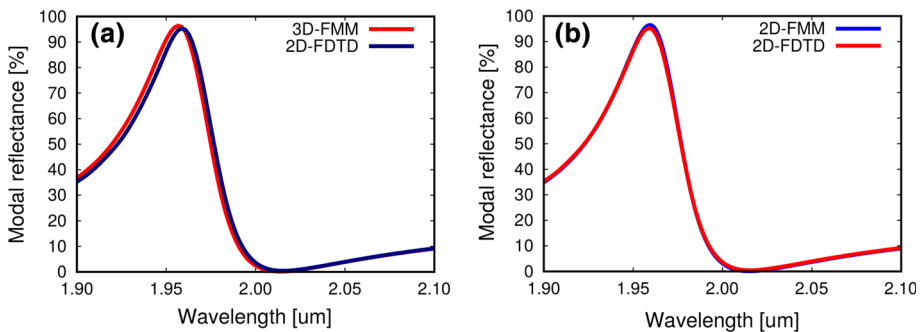


**Fig. 3** **a** Modal reflectances calculated by 2D FMM and 3D FMM for LMRG with resonance at 1960 nm. **b** Modal reflectances calculated by 2D FMM and 2D FDTD method. LMRG has period  $A = 1290 \text{ nm}$ ,  $f = 0.7$ ,  $h_1 = 200 \text{ nm}$  and  $h_2 = 710 \text{ nm}$

Both reflectance curves agree within 1.8% over the whole wavelength interval 1.9–2.1  $\mu\text{m}$  without any wavelength shift.

#### 4 Leaky-mode resonant grating optimization

We maximized the peak modal reflectance at a wavelength of 2000 nm using the 2D-FDTD method by varying the grating period  $\Lambda$ , groove depth  $h_1$ , waveguide layer thickness  $h_2$ , and fill factor  $f$ . Figure 4 shows how the spectral shape of modal reflectance is affected by parameters of the LMRG. The period  $\Lambda$  determines the wavelength at which the resonant coupling between the incident wave and the guided mode occurs. Variations in the period are manifested by almost pure resonant wavelength shifts. The groove depth variation  $h_1$  is related to the coupling strength. A substantial groove depth is necessary to achieve modal reflectances close to 100%. When close to the optimum point, the groove depth influences the reflectance peak shape. The thickness of the waveguide layer  $h_2$  has a direct impact on the guided mode. The fill factor determines the superstrate effective index and has a major impact on the properties of the waveguide as well. Variations in both these parameters have strong influence on the resonance wavelength and peak modal reflectance. Figure 5 shows effects which the fill factor has on the modal reflectance peak height, wavelength, and width. The modal reflectance reaches a maximum value of 96% for a fill factor of 0.62. The full width at half maximum (FWHM) of the modal reflectance peak decreases with increasing fill factor, while the resonance wavelength increases. Further, the influence of the number of grating grooves on the peak modal reflectance is shown in

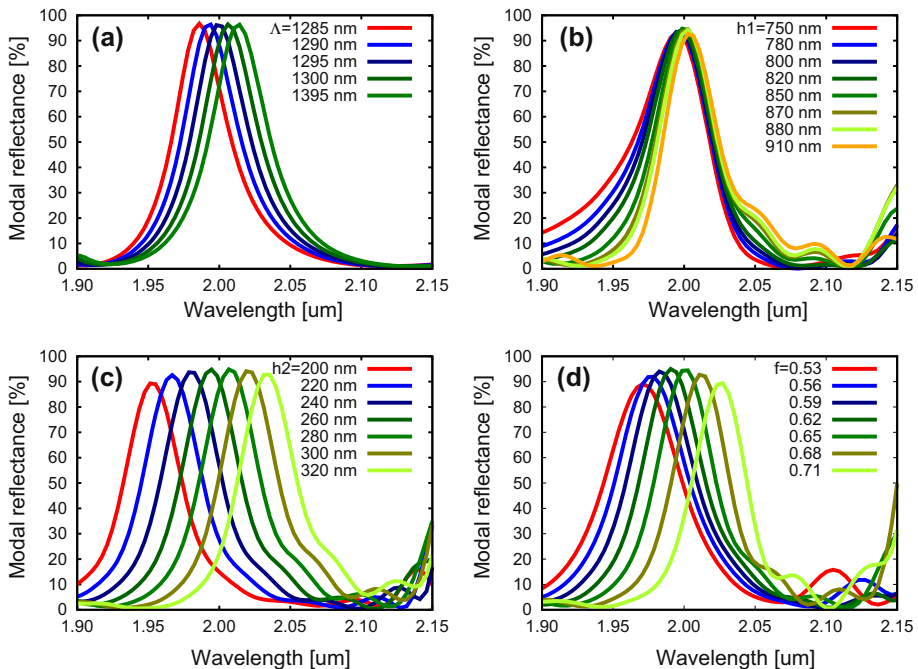


**Fig. 4** Dependence of the spectral shape of modal reflectivity on **a** grating period  $\Lambda$ , **b** grating groove depth  $h_1$ , **c** guiding layer thickness  $h_2$ , **d** grating fill factor  $f$

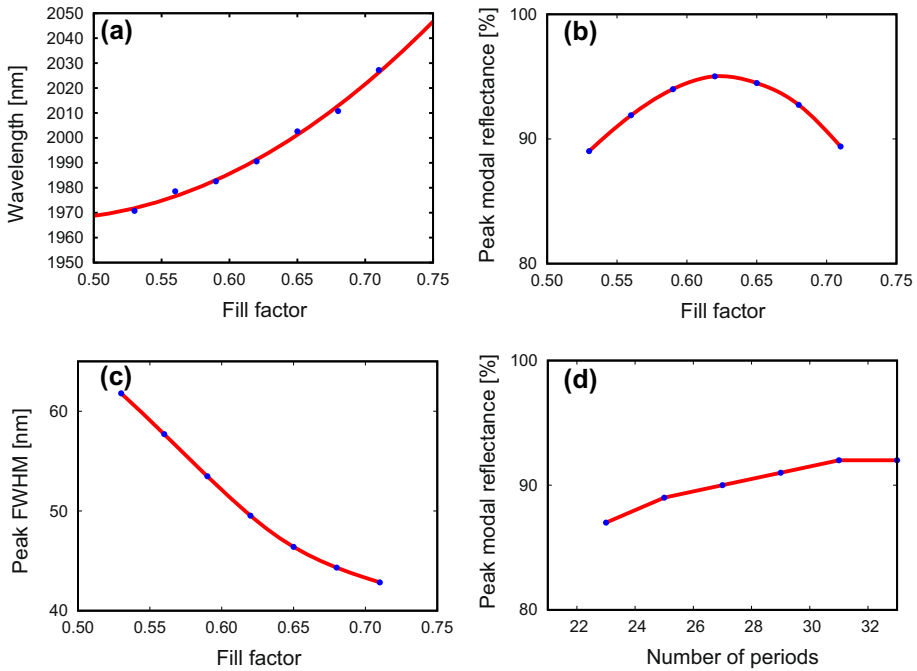


**Fig. 5** Dependence of the modal reflectance peak **a** wavelength, **b** height, **c** width on the fill factor **f**. **d** Dependence of the peak modal reflectance on the number of grooves of the truncated grating

Fig. 5d. It shows that the grating size should be much larger than the fibre core diameter, at least  $40\ \mu\text{m} \times 40\ \mu\text{m}$  for a fibre with a  $25\text{-}\mu\text{m}$  core diameter. The optimum parameters are summarised in the Table 2. The modal reflectance reaches a value of 96% for TE mode, while it remains as low as 1.6% for TM mode. The polarization extinction ratio achieves a value of 17.8 dB.

### 5 Fabrication tolerance analysis

In the previous section we focused on the search for optimum LMRG parameters. We also showed how the modal reflectance is influenced by deviations of various parameters from their optimum values. Now we will examine imperfections that may arise in diffraction gratings made by the FIB technique. We assume that the groove depth and fill factor have the normal distribution about their mean values with standard deviation  $\sigma$ . Ten realizations of the LMRG with random groove depths and constant fill factor were generated for each standard deviation shown in Fig. 6a. The spectral dependence of modal reflectance was

**Table 2** Optimum parameters of the LMRG

$\Lambda$ (nm)	1295	$h_1$ (nm)	860	$h_2$ (nm)	270	$f$	0.62
----------------	------	------------	-----	------------	-----	-----	------

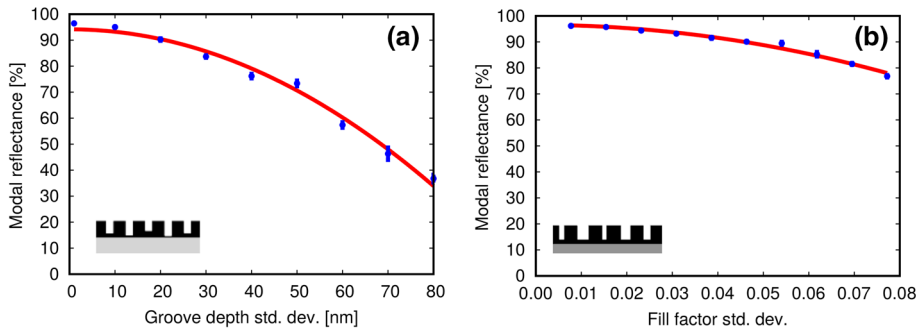


**Fig. 6** Effects of the **a** groove depth  $h_1$  and **b** fill factor  $f$  variance on the modal reflectance peak

calculated for each of these random gratings by the 2D-FDTD method. The same process was repeated with random fill factors and constant groove depth. Averaged peak modal reflectances are shown together with error bars in Fig. 6 for various standard deviations of corresponding parameters. We can conclude that standard deviations of the fill factor equal to 0.075, or of groove depth equal to 38 nm cause a decrease in the modal reflectance from 96 to 80%. The peak modal reflectance is expected to be 64% when both parameters change randomly with such standard deviations. We analysed also influence of rounded upper edges and trapezoidal shape of the grating grooves on the modal reflectance. We found these imperfections to be far less important compared to the groove depth and fill factor. These results should be taken into account when selecting the FIB milling parameters.

## 6 Conclusions

High-reflectance polarization-sensitive wavelength filters based on leaky-mode resonant gratings designed for the fabrication on the facet of optical fibres were numerically investigated. Such structures can be milled by focused ion beam in a high-refractive-index layer deposited on the fibre facet. In simulations, we used the 2D FDTD method, 2D FMM and 3D FMM. All these methods yielded almost identical results. We predicted that a modal reflectance peak height of 96% and bandwidth of about 50 nm for gratings centred at 2000 nm can be obtained for an optimised leaky-mode resonant diffraction grating fabricated in a tantalum layer. The polarization extinction ratio of 17.8 dB is sufficiently high to maintain the well-defined linear polarization of the laser. It was found that the grating size should be larger than  $40 \mu\text{m} \times 40 \mu\text{m}$  for a fibre core diameter of  $25 \mu\text{m}$  to get such high reflectance. We analysed the influence of systematic errors in the layer thickness, grating fill factor, and groove depth. Examination of the effects of the variance of the fill factor and groove depth on the modal reflectance was also carried out. Based on this analysis we can conclude that the fabrication of such leaky-mode gratings is feasible. Experimental work is under way, however it is beyond the scope of the present paper.

**Acknowledgements** The authors gratefully acknowledge support from the Czech Science Foundation under Grant No. GAP15-07908S. They also thank to Ardavan F. Oskooi, David Roundy, Mihai Ibanescu, Peter Bermel, J. D. Joannopoulos, and Steven G. Johnson for copylefting the Meep software under the GNU General Public Licence.



**Open Access** This article is distributed under the terms of the Creative Commons Attribution 4.0 International License (<http://creativecommons.org/licenses/by/4.0/>), which permits unrestricted use, distribution, and reproduction in any medium, provided you give appropriate credit to the original author(s) and the source, provide a link to the Creative Commons license, and indicate if changes were made.

## References

- Čtyroký, J.: 3-D bidirectional propagation algorithm based on Fourier series. *J. Lightwave Technol.* **30**(23), 3699–3708 (2012). <https://jlt.osa.org/abstract.cfm?URI=jlt-30-23-3699>
- Gissibl, T., Schmid, M., Giessen, H.: Spatial beam intensity shaping using phase masks on single-mode optical fibers fabricated by femtosecond direct laser writing. *Optica* **3**(4), 448–451 (2016a). <https://doi.org/10.1364/OPTICA.3.000448>
- Gissibl, T., Thiele, S., Herkommer, A., Giessen, H.: Sub-micrometre accurate free-form optics by three-dimensional printing on single-mode fibres. *Nat. Commun.* **7**, 11763, 1–9 (2016b). <https://doi.org/10.1038/ncomms11763>
- Golubenkov, G.A., Svakhin, A.S., Sychugov, V.A., Tishchenko, A.V.: Total reflection of light from a corrugated surface of a dielectric waveguide. *Sov. J. Quant. Electron.* **15**(7), 886–887 (1985). <http://stacks.iop.org/0049-1748/15/i=7/a=L02>
- Hessel, A., Oliner, A.A.: A new theory of wood's anomalies on optical gratings. *Appl. Opt.* **4**(10), 1275–1297 (1965). <https://doi.org/10.1364/AO.4.001275>
- Johnson, E.G., Stack, J., Suleski, T.J., Koehler, C., Delaney, W.: Fabrication of micro optics on coreless fiber segments. *Appl. Opt.* **42**(5), 785–791 (2003). <https://doi.org/10.1364/AO.42.000785>
- Johnson, E.G., Li, Y., Woodward, R., Poutous, M., Raghu, I., Shori, R.: Guided mode resonance filter as wavelength selecting element in er: ZBLAN fiber laser. In: Advanced Photonics Congress, Optical Society of America, p STu3F.1 (2012). <https://doi.org/10.1364/SOF.2012.STu3F.1>
- Kanamori, Y., Okochi, M., Hane, K.: Fabrication of antireflection subwavelength gratings at the tips of optical fibers using UV nanoimprint lithography. *Opt. Express* **21**(1), 322–328 (2013). <https://doi.org/10.1364/OE.21.000322>
- Kostovski, G., White, D., Mitchell, A., Austin, M., Stoddart, P.: Nanoimprinted optical fibres: Biotemplated nanostructures for SERS sensing. *Biosensors and Bioelectronics* **24**(5), 1531–1535 (2009). <https://doi.org/10.1016/j.bios.2008.10.016> (selected Papers from the Tenth World Congress on Biosensors Shanghai, China, May 14–16, 2008)
- Kowalczyk, M., Haberko, J., Wasylczyk, P.: Microstructured gradient-index antireflective coating fabricated on a fiber tip with direct laser writing. *Opt. Express* **22**(10), 12545–12550 (2014). <https://doi.org/10.1364/OE.22.012545>
- Lalanne, P., Hugonin, J.P.: High-order effective-medium theory of subwavelength gratings in classical mounting: application to volume holograms. *J. Opt. Soc. Am. A* **15**(7), 1843–1851 (1998). <https://doi.org/10.1364/JOSAA.15.001843>
- MacLeod, B.D., Hobbs, D.S., Sabatino III, E.: Moldable AR microstructures for improved laser transmission and damage resistance in CIRCUM fiber optic beam delivery systems. **8016**, 80160Q, 1–14 (2011). <https://doi.org/10.1117/12.883281>
- Mashev, L., Popov, E.: Zero order anomaly of dielectric coated gratings. *Opt. Commun.* **55**(6), 377–380 (1985). [https://doi.org/10.1016/0030-4018\(85\)90134-8](https://doi.org/10.1016/0030-4018(85)90134-8)
- Mehta, A.A., Rumpf, R.C., Roth, Z.A., Johnson, E.G.: Guided mode resonance filter as a spectrally selective feedback element in a double-cladding optical fiber laser. *IEEE Photonics Technol. Lett.* **19**(24), 2030–2032 (2007)
- Neviere, M., Petit, R., Cadilhac, M.: About the theory of optical grating coupler-waveguide systems. *Opt. Commun.* **8**(2), 113–117 (1973). [https://doi.org/10.1016/0030-4018\(73\)90150-8](https://doi.org/10.1016/0030-4018(73)90150-8)
- Oskooi, A.F., Roundy, D., Ibanescu, M., Bermel, P., Joannopoulos, J.D., Johnson, S.G.: MEEP: a flexible free-software package for electromagnetic simulations by the FDTD method. *Comput. Phys. Commun.* **181**, 687–702 (2010). <https://doi.org/10.1016/j.cpc.2009.11.008>
- Prasciolu, M., Cojoc, D., Cabrini, S., Businaro, L., Candeloro, P., Tormen, M., Kumar, R., Liberale, C., Degiorgio, V., Gerardino, A., Gigli, G., Pisignano, D., Fabrizio, E.D., Cingolani, R.: Design and fabrication of on-fiber diffractive elements for fiber-waveguide coupling by means of e-beam lithography. *Microelectron. Eng.* **67–68**, 169–174 (2003). [https://doi.org/10.1016/S0167-9317\(03\)00068-6](https://doi.org/10.1016/S0167-9317(03)00068-6) (proceedings of the 28th International Conference on Micro- and Nano-Engineering)

- Sanghera, J., Florea, C., Busse, L., Shaw, B., Miklos, F., Aggarwal, I.: Reduced fresnel losses in chalcogenide fibers by using anti-reflective surface structures on fiber end faces. *Opt. Express* **18**(25), 26760–26768 (2010). <https://doi.org/10.1364/OE.18.026760>
- Schiappelli, F., Kumar, R., Prasciolu, M., Cojoc, D., Cabrini, S., Vittorio, M.D., Visimberga, G., Gerardino, A., Degiorgio, V., Fabrizio, E.D.: Efficient fiber-to-waveguide coupling by a lens on the end of the optical fiber fabricated by focused ion beam milling. *Microelectron Eng.* **73–74**, 397–404 (2004). <https://doi.org/10.1016/j.mee.2004.02.077>. (micro and Nano Engineering 2003)
- Sharon, A., Rosenblatt, D., Friesem, A.A.: Resonant grating-waveguide structures for visible and near-infrared radiation. *J. Opt. Soc. Am. A* **14**(11), 2985–2993 (1997). <https://doi.org/10.1364/JOSAA.14.002985>
- Sims, R.A., Roth, Z.A., Willis, C.C.C., Kadwani, P., McComb, T.S., Shah, L., Sudesh, V., Poutous, M., Johnson, E.G., Richardson, M.: Spectral narrowing and stabilization of thulium fiber lasers using guided-mode resonance filters. *Opt. Lett.* **36**(5), 737–739 (2011). <https://doi.org/10.1364/OL.36.000737>
- Vanek, M., Vanis, J., Baravets, Y., Todorov, F., Ctyroky, J., Honzatko, P.: High-power fiber laser with a polarizing diffraction grating milled on the facet of an optical fiber. *Opt. Express* **24**(26), 30225–30233 (2016). <https://doi.org/10.1364/OE.24.030225>
- Williams, H.E., Freppon, D.J., Kuebler, S.M., Rumpf, R.C., Melino, M.A.: Fabrication of three-dimensional micro-photonics structures on the tip of optical fibers using SU-8. *Opt. Express* **19**(23), 22910–22922 (2011). <https://doi.org/10.1364/OE.19.022910>
- Yang, X., Ileri, N., Larson, C.C., Carlson, T.C., Britten, J.A., Chang, A.S.P., Gu, C., Bond, T.C.: Nanopillar array on a fiber facet for highly sensitive surface-enhanced raman scattering. *Opt. Express* **20**(22), 24819–24826 (2012). <https://doi.org/10.1364/OE.20.024819>